CHEMISTRY
AN ASIAN JOURNAL

DOI: 10.1002/asia.201100882

Biomimetic Graphene Surfaces with Superhydrophobicity and Iridescence

Jian-Nan Wang,[a] Rui-Qiang Shao,[a] Yong-Lai Zhang,*[a] Li Guo,[a] Hao-Bo Jiang,[b] Dong-Xiao Lu,[b] and Hong-Bo Sun*[a, b]

Triggered by the fantastic functions and bright appearance of biological systems in nature, enormous efforts have been devoted to biomimetic fabrication. For instance, butterfly wings[1–3] and red rose petals[4–7] have attracted increasing attention due to their excellent water repellency and splendid structural color. Consequently, colorful superhydrophobic surfaces have become a hot topic with significance in both fundamental research and practical applications.[8–10] Previous studies have shown that hierarchical micro-/nanostructures on biosurfaces play a critical role in the multifunctional acquisition. On the one hand, the highly rough textures trap a wealth of air bubbles at the interface preventing a water droplet from spreading; thus, the surfaces exhibit a high water contact angle (CA > 150°). Along this line, a variety of water-repellent surfaces with multiscale structures have been achieved by classical "top-down" and "bottom-up" approaches.[9–13] On the other hand, as inspired by many natural species that use structural color as a warning or protection,[2,7,14–16] the surface microstructures are not randomly distributed but rigidly arranged in periodic micro-patterns, and therefore triggered light diffraction and scattering contribute to the brilliant appearance. However, due to technical challenges in the fabrication of uniform and well-defined nanostructures in the long-range order, most of the superhydrophobic surfaces hardly show any structural color. To date, only a few attempts to such multifunctional surfaces have been realized. For instance, Gu et al.[1] fabricated colloidal photonic crystal films with both structural color and superhydrophobicity at the cost of long time and high temperature. Jiang et al.[17] reported multicolor superhydrophobic coatings that depend on metal ions for the appearance of color; in their study, individual samples exhibited a single color. Wu et al.[18] fabricated superhydrophobic surfaces with iridescence by employing multiple procedures including interference, surface modification, and chemical plating. Consequently, a facile and convenient approach for surfaces with superhydrophobicity and iridescent structural color is in urgent need.

Unlike the classical slippery superhydrophobic surface represented by the famous self-cleaning lotus leaf, rose petals possess a sticky superhydrophobicity,[6] exhibiting both a high water contact angle (CA > 150°) and strong adhesion. Because of the adhesive force, flowers are able to maintain a fresh appearance, as a water droplet cannot roll off effortlessly but stays stably on the surface without any movement. To date, by tailoring the chemical composition,[19–20] the geometrical structure,[21–23] or interfacial capillary[24] and van der Waals forces,[25] superhydrophobic surfaces with high adhesion were successfully prepared. Due to their representativeness in wetting behavior and their research value in various realms,[11–13] such as liquid transportation in microfluidic systems and biomedical applications, high-adhesion surperhydrophobic surfaces become increasingly important.

Recently, graphene has attracted much attention due to its unique single atom-layer structure, which contributes to its wide applications[26] in nanoelectronics, sensing devices, energy storage, and even tissue engineering. For example, graphene has proven to be a promising biocompatible scaffold that could accelerate the specific differentiation of human mesenchymal stem cells (hMSCs) into bone cells.[27] In this case, the cell adhesion on the graphene surface plays a critical role in the long-term differentiation;[28] therefore, a precise control of the surface wettability of graphene becomes a significant issue. Generally, superhydrophobic graphene substrates could be fabricated by using an irregular stack of graphene oxides (GO) prepared by chemical oxidation of graphite. In this procedure, to reduce the surface energy, the hydrophilic oxygen-containing groups on the GO surface have to be removed beforehand.[29,30] To the best of our knowledge, modulation of the wetting property of graphene by micro-/nanostructuring and simultaneous control of chemical composition have not been realized. Moreover, despite the pioneering biomimetic fabrications of periodic micro-/nanostructures based on a wide range of materials, a bioinspired graphene surface with properties comparable to natural surfaces has not been reported yet.

[a] J.-N. Wang, R.-Q. Shao, Dr. Y.-L. Zhang, L. Guo, Prof. H.-B. Sun
State Key Laboratory on Integrated Optoelectronics
College of Electronic Science and Engineering
Jilin University
2699 Qianjin Street, Changchun 130012 (P. R. China)
Fax: (+86) 431-85168281
E-mail: yonglaizhang@jlu.edu.cn
hbsun@jlu.edu.cn

[b] H.-B. Jiang, D.-X. Lu, Prof. H.-B. Sun
College of Physics
Jilin University
2699 Qianjin Street, Changchun 130012 (P. R. China)

Supporting information for this article is available on the WWW under http://dx.doi.org/10.1002/asia.201100882.

With a concept inspired by butterfly wings and rose petals, we report here a simple one-step method to generate superhydrophobic graphene surfaces with high adhesion and bright structural color, which we call biomimetic graphene surfaces. Two-beam laser interference was utilized to fabricate periodic grating structures and to simultaneously remove the oxygen groups on the GO film. Notably, this method allows realization of three unique features at the same time: 1) formation of hierarchical structures (grating microstructure and layered nanostructure); 2) modulation of the chemical composition; and 3) attainment of structural color. To sum up, we obtained native graphene-based superhydrophobic surfaces with high adhesion and brilliant color in an easy, effective, and controllable way.

Figure 1a shows schematically the two-beam laser interference fabrication of a graphene biomimetic surface. A laser beam of 355 nm wavelength was split into two branches and guided to interfere directly on the surface of a GO film. After 10 seconds of laser exposure, typical grating micropatterns with a period of 2 μm were formed (left image in Figure 1a). Interestingly, as directly observed by the naked eye, the as-prepared graphene surfaces took on a wonderful iridescent appearance throughout the exposed area matching the shape of the round laser spot (right image in Figure 1a), The iridescence may originate from the diffraction of the grating, which can be expressed as $m\lambda = d(\sin\theta_D - \sin\theta_I)$, in which m is the diffraction order, d is the period of the grating, and θ_D and θ_I are the diffraction and incident angles, respectively. Thus, for a given viewing angle (or θ_I), the diffracted light of a different wavelength occupies a distinct space (or θ_D), and the chromatic dispersion gives rise to a color separation ranging from purple to red, like a rainbow. Furthermore, scanning electron microscopy (SEM) images demonstrate the morphological details of the prepared samples. A uniform grating feature is clearly observed at low magnification (Figure 1b). However, at high magnification, unique secondary textures at the borders of the gratings in the form of dense nanofolders and tiny nanovilli can be observed (Figure 1c). This layered nanostructure may result from the structural feature of graphene oxide (GO), which is a stack of individual GO sheets. When the laser beam came into contact with the material, ablation proceeded along with the interference process. GO was spattered out where the distributed energy was high, and an interior stack was exposed. Finally, due to the cooperation of the above-mentioned factors, dual-sized composite textures formed without further post-treatment.

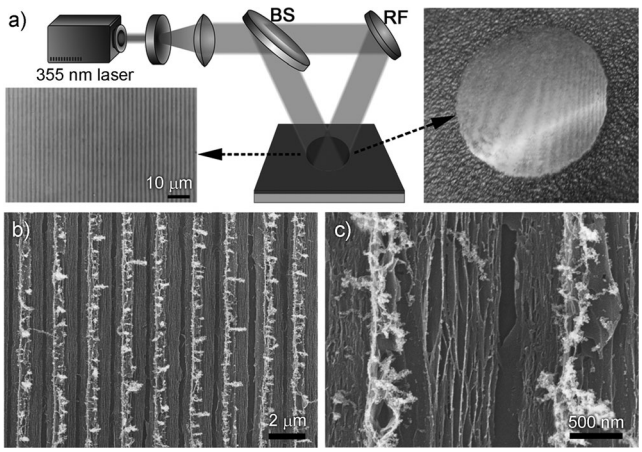

Figure 1. a) Fabrication scheme of biomimetic graphene surfaces by two-beam laser interference. The image on the left is an optical microscope image, and the one on the right is a photograph of the graphene surface with iridescence (see the Supporting Information for the color version of this image). BS, beam splitter; RF, reflector. b) SEM image of the grating structure of the graphene surface fabricated at 0.3 W. c) Magnified SEM image. The layered nanostructure can easily be identified from the image.

Because the ablated area formed a concave part and determined the final morphology, we can adjust the surface pattern by tuning up the laser intensity. As presented in Figure 2a, the surface texture changed obviously with the laser intensity. The pristine GO surface was very smooth; only some wrinkles could be identified from the image. When the laser beam of 0.15 W was split into two branches and interfered on the surface of GO, a striped pattern appeared. As the laser intensity increased, the laser–solid interaction strengthened, gradually extending from the top to the interior layers. Accordingly, more inner laminar borders appeared, and the plateau area after the ablation became narrower. Finally, the entire surface participated in the reaction, and nanostructures wrapped the top and side of the gratings.

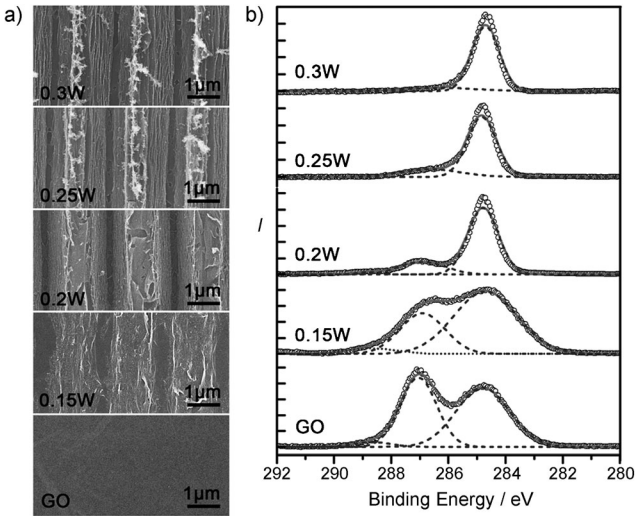

Figure 2. a) SEM images of the grating structure of the graphene surface fabricated at different output power. b) C1s XPS spectra of pristine GO and GO films after two-beam laser interference treatment at different laser power. The spectra have been offset along the vertical axis for clarity.

Not only the surface topography, but also the chemical composition changed during the laser process, as the analysis of the C1s peak by X-ray photoelectron spectroscopy (XPS) revealed (Figure 2b). When the laser power was increased, the peaks at 286.9 eV and 288.8 eV corresponding

to the C–O and C=O contents decreased, while the peak of C–C at 284.8 eV increased, thus indicating the removal of oxygen-containing groups.[31,32] The laser-induced reduction reached the largest extent at 0.3 W, as evidenced by the near disappearance of the C–O and C=O peaks and the maximum intensity observed for the C–C peak. In our experiments, the oxygen contents in the GO film could be modulated in the range of 5.4–35.2% (see Figure S1 in the Supporting Information). As the percentage of oxygen groups decreased sharply and thus changed the hydrophilic nature of the material, an additional process of low-energy modification was unnecessary. In addition, the laser-reduced GO was very stable and its surface properties did not change after long time storage at ambient conditions.

According to the discussion above, the one-step process endows the surface with multi-scale roughness and a significantly decreased surface energy, which makes it promising for the superhydrophobicity. To gain further insight into its wetting property, we performed contact angle (CA) measurements in directions parallel and perpendicular to the grating. As shown in Figure 3a, before laser exposure, the

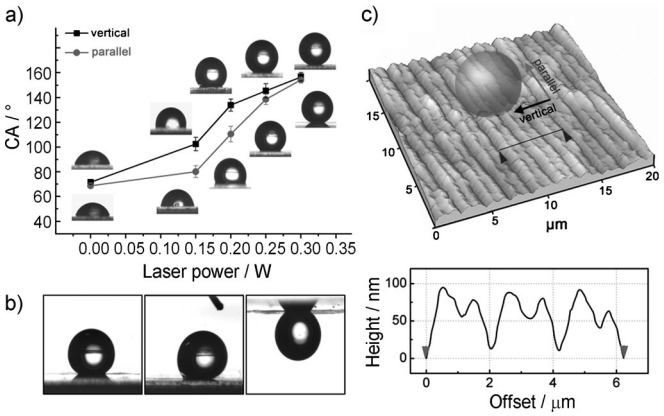

Figure 3. a) Dependence of the CA on the laser power in both vertical and parallel directions of the grating structure. Photographic images of a water droplet on the different substrates have been inserted. b) Images of a water droplet on a flat and tilted biomimetic graphene surface. Tilt angles (from left to right) are 0°, 45°, and 180°, respectively. c) 3D-AFM image of the biomimetic graphene substrate and the corresponding height profile plot.

flat surface has a low CA of 68.7°, thus indicating its weak hydrophilicity. However, after the treatment, the measured CA increased monotonically with increasing laser power, and finally reached a value of 156.7°, thereby illustrating the transition to superhydrophobicity. In addition, the CA anisotropy decreased with the increase in the laser power so that ultimately isotropic superhydrophobicity was obtained. The results showed that the water CA can be regulated by varying the density of the hydrophilic microdomain and by tuning the surface topography.

Based on the understanding that the contact angle hysteresis (the difference between the advancing contact angle and the receding angle) or sliding angle is a direct assessment of adhesion, we tested the behaviors of water droplets on inclined surfaces, as shown in Figure 3b. Based on the aforementioned experiments, we performed measurements with the sample processed at 0.3 W. When the surface was tilted at 45°, the CA at the front was much larger than that at the back. However, even when the surface was turned upside down, the water droplet was firmly pinned to the surface, thus indicating the strong adhesion at the interface. As the volume of the droplet was 4 μL, the adhesive force was estimated to be at least 40 μN in order to balance gravity. Therefore, the prepared surface possessed both an excellent water resistance and a high adhesive force.

As previously reported, Wenzel's and Cassie's models are the two basic theories used to explain the micromechanism of the wetting behavior on superhydrophobic surfaces. In the former model, the rough surface is completely filled with water and displays a strong interaction with water but has a relatively low CA. By contrast, in the latter model, air pockets trapped in the valley force water to touch only the sharp tips, and the surface exhibits a very high CA but ultralow friction. In our samples, the height of the structure was only approximately 80 nm, as determined by atomic force microscopy (Figure 3c). Allowing for a grating period of 2 μm, it can be conferred that water droplets would enter into the microscale grooves and wet the bottom of the low and wide structure. However, the folders on the side and filaments on the top will prevent water from intruding into the nanoscale spaces, and thus correspond to a Cassie impregnating wetting regime.[6] As it provides intimate contact over a large area and a certain roughness at the same time, the contact mode has the potential for both strong adhesion and high CA. Consequently, a water droplet could be suspended on the inverted surface where it maintained a spherical shape.

In addition to the surface topography, the chemical heterogeneity affected the wetting behavior. The CAs in the parallel direction were smaller than those in the perpendicular direction. As the barrier potential caused by the grating depths is weak, the wetting anisotropy can be explained by considering the chemical hybrid of the surface. The hydrophilic stripes on the top which first come into contact with the droplet generate a strong attraction and induce the droplet to extend along the grating, while the hydrophobic areas prevent water from spreading in the perpendicular direction. As a result, the surface shows an anisotropic wetting behavior.

In summary, biomimetic graphene surfaces with both superhydrophobicity and iridescence were prepared through a facile interference technique. Periodic grating micropatterns and nanoscale layered structures formed during the laser-induced removal of hydrophilic oxygen groups, which contributes to the superhydrophobic and colorful features. Moreover, the resultant graphene surfaces showed a unique high adhesion, which is promising for applications of water transport, analysis of small volumes of liquid samples, and in microfluidic devices. The results not only provide new insights into the design of colorful superhydrophobic surfaces, but

are also beneficial for our understanding of interactions at the liquid–graphene interface.

Experimental Section

Materials and Sample Fabrication

GO was prepared from purified natural graphite (Aldrich, $<150\,\mu m$) by following Hummers' method. The as-synthesized GO was dispersed into individual sheets in distilled water at a concentration of $3\,mg\,mL^{-1}$ with the aid of ultrasound. Glass substrates were cleaned with acetone, absolute ethanol, and deionized water. GO was spin-coated onto the slides at 1000 rpm and dried to evaporate the solvent. Then, a frequency-tripled, Q-switched, single-mode Nd:YAG laser (Spectra-Physics) with about 10 ns pulse width ($\lambda = 355$ nm; beam size ca. 9 mm in diameter) was split into two beams with the same optical path length to the sample. Superhydrophobic surfaces were created by laser interference.

Instrumentation

The CA measurements were made by using the Contact Angle System OCA 20 (DataPhysics Instruments GmbH, Germany) at ambient temperature. The CAs were measured by the sessile-drop method with a water droplet of 4 μL. SEM images were obtained by using a field-emission scanning electron microscope (JSM-7500F, JEOL, Japan). X-ray photoelectron spectroscopy (XPS) was performed using an ESCALAB 250 spectrometer. Atomic force microscopy (AFM) micrographs were obtained using a NanoWizard II BioAFM instrument (JPK Instruments AG, Berlin, Germany) in the tapping mode.

Acknowledgements

This work was supported by the National Science Foundation of China (Grant 61008014) and 973 Program (Grant 2011CB013005). We also acknowledge the China Postdoctoral Science Foundation (Grants 20110490156 and 201104522) and the Hong Kong Scholar Program XJ2011014.

Keywords: adhesion · graphene · hydrophobic effect · laser interference · surface chemistry

[1] Z. Z. Gu, H. Uetsuka, K. Takahashi, R. Nakajima, H. Onishi, A. Fujishima, O. Sato, *Angew. Chem.* **2003**, *115*, 922–925; *Angew. Chem. Int. Ed.* **2003**, *42*, 894–897.
[2] P. Vukusic, J. R. Sambles, *Nature* **2003**, *424*, 852–855.
[3] Y. Zheng, X. Gao, L. Jiang, *Soft Matter* **2007**, *3*, 178–182.
[4] M. K. Dawood, H. Zheng, T. H. Liew, K. C. Leong, Y. L. Foo, R. Rajagopalan, S. A. Khan, W. K. Choi, *Langmuir* **2011**, *27*, 4126–4133.
[5] J. Xi, L. Jiang, *Ind. Eng. Chem. Res.* **2008**, *47*, 6354–6357.
[6] L. Feng, Y. Zhang, J. Xi, Y. Zhu, N. Wang, F. Xia, L. Jiang, *Langmuir* **2008**, *24*, 4114–4119.
[7] L. Feng, Y. Zhang, M. Li, Y. Zheng, W. Shen, L. Jiang, *Langmuir* **2010**, *26*, 14885–14888.
[8] O. Sato, S. Kubo, Z. Z. Gu, *Acc. Chem. Res.* **2009**, *42*, 1–10.
[9] K. Liu, L. Jiang, *Nano Today* **2011**, *6*, 155–175.
[10] X. Zhang, F. Shi, J. Niu, Y. Jiang, Z. Wang, *J. Mater. Chem.* **2008**, *18*, 621–633.
[11] X. Feng, L. Jiang, *Adv. Mater.* **2006**, *18*, 3063–3078.
[12] L. Feng, S. Li, Y. Li, H. Li, L. Zhang, J. Zhai, Y. Song, B. Liu, L. Jiang, D. Zhu, *Adv. Mater.* **2002**, *14*, 1857–1860.
[13] F. Xia, L. Jiang, *Adv. Mater.* **2008**, *20*, 2842–2858.
[14] P. Vukusic, J. R. Sambles, C. R. Lawrence, *Nature* **2000**, *404*, 457.
[15] P. Vukusic, J. R. Sambled, C. R. Lawrence, R. J. Wootoon, *Nature* **2001**, *410*, 36.
[16] A. R. Parker, V. L. Welch, D. Driver, N. Martini, *Nature* **2003**, *426*, 786–787.
[17] L. Chen, H. Meng, L. Jiang, S. Wang, *Chem. Asian J.* **2011**, *6*, 1757–1760.
[18] D. Wu, Q. D. Chen, H. Xia, J. Jiao, B. B. Xu, X. F. Lin, Y. Xu, H. B. Sun, *Soft Matter* **2010**, *6*, 263–267.
[19] N. Zhao, Q. Xie, X. Kuang, S. Wang, Y. Li, X. Lu, S. Tan, J. Shen, X. Zhang, Y. Zhang, J. Xu, C. C. Han, *Adv. Funct. Mater.* **2007**, *17*, 2739–2745.
[20] Y. Lai, C. Lin, J. Huang, H. Zhuang, L. Sun, T. Nguyen, *Langmuir* **2008**, *24*, 3867–3873.
[21] X. J. Huang, D. H. Kim, M. Im, J. H. Lee, J. B. Yoon, Y. K. Choi, *Small* **2009**, *5*, 90–94.
[22] Y. Lai, X. Gao, H. Zhuang, J. Huang, C. Lin, L. Jiang, *Adv. Mater.* **2009**, *21*, 3799–3803.
[23] Y. Yao, X. Dong, S. Hong, H. Ge, C. C. Han, *Macromol. Rapid Commun.* **2006**, *27*, 1627–1631.
[24] Z.-G. Guo, W. M. Liu, *Appl. Phys. Lett.* **2007**, *90*, 223111.
[25] M. Jin, X. Feng, L. Feng, T. Sun, J. Zhai, T. Li, L. Jiang, *Adv. Mater.* **2005**, *17*, 1977–1981.
[26] Q. Ji, I. Honma, S. M. Paek, M. Akada, J. P. Hill, A. Vinu, K. Ariga, *Angew. Chem.* **2010**, *122*, 9931–9933; *Angew. Chem. Int. Ed.* **2010**, *49*, 9737–9739.
[27] T. R. Nayak, H. Andersen, V. S. Makam, C. Khaw, S. Bae, X. Xu, P. L. R. Ee, J. H. Ahn, B. H. Hong, G. Pastorin, B. Ozyilmaz, *ACS Nano* **2011**, *5*, 4670–4678.
[28] S. Y. Park, J. Park, S. H. Sim, M. G. Sung, K. S. Kim, B. H. Hong, S. Hong, *Adv. Mater.* **2011**, *23*, H263–H267.
[29] J. Rafiee, M. A. Rafiee, Z. Z. Yu, N. Koratkar, *Adv. Mater.* **2010**, *22*, 2151–2154.
[30] X. Q. Zhang, S. H. Wan, J. B. Pu, L. P. Wang, X. Q. Liu, *J. Mater. Chem.* **2011**, *21*, 12251–12258.
[31] Y.-L. Zhang, L. Guo, S. Wei, Y.-Y. He, H. Xia, Q. D. Chen, H. B. Sun, F. S. Xiao, *Nano Today* **2010**, *5*, 15–20.
[32] Y.-L. Zhang, Q. D. Chen, H. Xia, H. B. Sun, *Nano Today* **2010**, *5*, 435–448.

Received: October 26, 2011
Published online: January 11, 2012

